# Introducing the NewLib Library and its application to multi-level, large-scale solar field models

Igor Belot<sup>1</sup>, François Nepveu<sup>2</sup>, Pierre Garcia<sup>1</sup>, Etienne Letournel<sup>1</sup>, Nathan Fournier<sup>1</sup>, Teddy Chedid<sup>1</sup>, Alexis Gonnelle<sup>1</sup>, Guillaume Raigné<sup>1</sup>, Pierre Delmas<sup>1</sup>

<sup>2</sup>CEA, CEA Tech Pays de la Loire, F-44340 Bouguenais, France, {francois.nepveu}@cea.fr

### **Abstract**

Solar thermal technology is a promising solution for decarbonizing heat production in industrial applications and district heating networks. When combined with heat storage and advanced control strategies, it can cover a significant share of heat demands. However, designing and optimizing such systems is complex due to their dynamic behavior and the interplay of multiple physical phenomena. To better understand and design these systems, dynamic modeling tools are essential.

Modelica is particularly well-suited for this purpose. At Newheat, large scale solar thermal field models have been developed in the *Modelica* language using the *Dymola* environment. These models represent the thermal and hydraulic behavior of a solar thermal field at two different levels of complexity. Each is designed for different project phases, fast simulations for early-stage feasibility studies and slower but more detailed simulations for the engineering phase.

To assess the accuracy of both models, comparisons with measured data on an operational solar plant were performed. Results indicate that both models achieve high thermal accuracy, with errors of less than 4% in annual heat production. On the hydraulic side, the detailed model provides more precise results than the simplified one. The main drawback of this model being slow simulations in case of very complex solar field layouts.

Moving forward, these models will support various applications and enable scalable modeling of complex solar thermal systems, adapting to different project phases and requirements.

Keywords: solar thermal, ThermoFluidStream library, conceptual design, detailed engineering

# 1 Introduction

Newheat is a renewable and sustainable heat supplier, offering innovative and tailor-made solutions for major heat consumers worldwide: industrial sites and district heating networks. Its activity is to develop, design, build, finance and operate renewable heat plants, which can combine waste heat recovery, solar thermal, short and long-term thermal storage systems, optimized electrification solutions (industrial heat pumps, etc...) and, if necessary, combustion of renewable resources. The company currently has 6 sites in operation for a total of 40 MW of solar thermal fields installed.

Dynamic models of renewable heat components and plants are needed to estimate the performances and cost of the systems, and finally to assess the heat price defined in heat supply contracts over 15 to 25 years.

In the upstream phase of project development (conceptual design phase), models are used to explore all possible renewable heat production system configurations. The energy mix is not yet fixed, and an expected heat price must be assessed for several heat producer configurations, storage facilities and heat delivery points.

In the detailed engineering phase, dynamic models of complete systems are used for the detailed design of projects based on technical and economic criteria. At this stage, the hydraulic configuration of the installation and associated operating procedures (high-level control) are finalized, components are selected and specified, and location or implementation constraints (distances, soil, environment, etc.) are integrated.

NewLib models can also be used later in the construction phase to improve the Factory Acceptance Tests of the Programmable Logic Control when received, during commissioning to help tune the parameters of the controllers, and finally in operation as digital twins to detect and diagnose faults.

In this paper, simple solar thermal field models used for conceptual design and more detailed models used for engineering needs are presented, compared, and validated against measured data from large scale solar thermal plants. After the presentation of the context and objectives in the present section, the rest of the paper is organized as follows:

- Section 2 presents the NewLib library, within the *Dymola* Environment, dedicated to the dynamic simulation of components and renewable heat production plants.
- Section 3 introduces the core of the NewLib library with special focuses on the media, pipe, heat exchanger and solar field models.
- Section 4 presents comparison results between NewLib models at 2 levels of details with measurements obtained from an operating solar plant.
- Section 5 summarizes the main messages of the present article and gives perspectives for the development roadmap regarding the NewLib library.

# 2 Presentation of the library

## 2.1 Overall presentation

Newheat has developed an in-house proprietary library called NewLib within the *Dymola* Environment, for internal purposes. It is not intended for public distribution or commercial release now. This *Modelica* Library:

- Is dedicated to the dynamic simulation of components and renewable heat production plants.
- Includes renewable heat components, control blocks and systems, tailored to the needs of its commercial projects.
- Provides multiple complexity levels of modeling for components, subsystems, materials, and fluids.
- Includes standardized interfaces enabling the interchangeability of component models of the same type in a system model.
- Enables annual simulations of renewable thermal plants within a few minutes (conceptual design phase).
- Uses the DASSL and CVODE solvers within the *Dymola* environment.

After benchmarking various thermofluidic libraries in the *Modelica* language – including the *MSL*, *IBPSA*, *Liquid Cooling*, *Thermal Power* and *ThermalSystems* – based on qualitative criteria as the library targeted industrial sector, the fluid port approach, the available media and the availability of models relevant to Newheat's need, as well

as more quantitative KPIs like computation time and success rate of simulation in a parametric study, the *ThermoFluidStream* (*TFS*) library (Zimmer et al., 2022) was selected as a basis for the NewLib library, for the following reasons: Easy to use; Adequacy to Newheat's present and future needs; Robustness: based on an innovative numerical calculation scheme (Zimmer, 2020), designed to be robust even on complex thermo-fluid architectures; Fluid representation: partially compatible with the *Modelica* standard fluid library (MSL. Media).

The NewLib library is actively developed on *GitlLab*, therefore a methodology of continuous integration based on non-regression tests using the *Testing* library from Dassault (Hammond-Scott, 2022) is being followed.

### 2.2 Structure

The NewLib library is structured on packages as depicted in **Figure 1**. The core packages are the Components, Control and Media packages.

The Components package contains models of varying complexity representing the main components of a renewable thermal plant. These include producers such as solar fields, boilers and heat pumps; storage systems such as TTES (Tank Thermal Energy Storage), PTES (Pit Thermal Energy Storage), and BTES (Borehole Thermal Energy Storage); heat exchangers, including liquid/liquid plate heat exchangers and liquid/moist air finned-tube heat exchangers... Some of these models are largely inspired by other open-source libraries, such as *IBPSA* (Wetter, 2022). More specific models, including solar field models, will be described in more detail in this paper.

The Control package contains the models of the two levels of control commonly found in renewable heat plants. High-level control (HLC): 1. defines the conditions to enter and exit the different operating modes of the plants (and associated configuration of actuators) based on the different data acquisition made on site. For example, the operating modes of the solar field are standby, preheating, production, overheating prevention and overheating. In NewLib, the Modelica StateGraph2 library (Olsson, 2020) is used to develop the models of the HLC closely reflecting those implemented in operational plants; 2. defines the setpoints to be achieved by the Low-level control (LLC). LLC is responsible for applying and maintaining the setpoints defined by HLC. In practice, this typically involves regulation techniques, such as PID control. In NewLib, to ensure fast simulations, a modelbased approach is used through an open loop control strategy. First-order filters are added to the command to eliminate nonlinear equations.

The Media package: Media models must be numerically robust, to avoid errors during dynamic simulations, as well as fast, accurate, and capable of computing the thermodynamic and transport fluid properties over a wide range of temperatures (and potentially pressures).

Currently, only a monophasic and incompressible liquid model based on a polynomial formulation is available. This model has been extended to represent antifreeze and thermal oil heat transfer fluids from properties data as a function of the temperature to determine the corresponding polynomial coefficients.

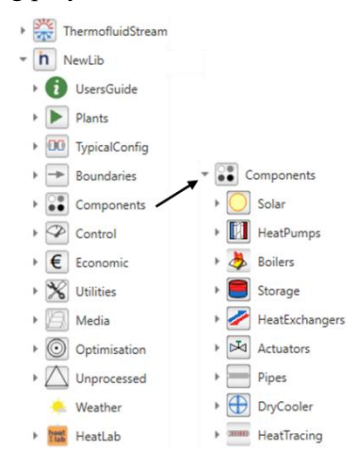
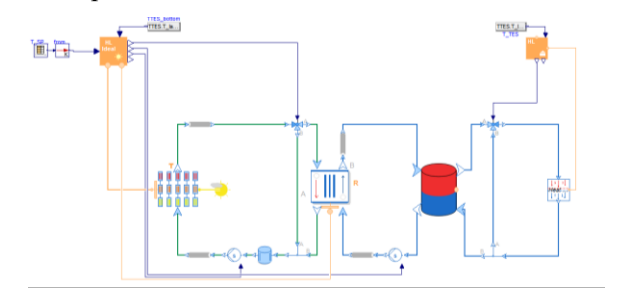


Figure 1. Packages of the NewLib library

# 2.3 The subsystem approach in NewLib

As part of Newheat strategic vision, NewLib library aims to provide a comprehensive framework – usable by Newheat's non-developer engineers – to all simulation requirements, from the conceptual design phase to the operational phase. Indeed, a Component-by-Component modeling approach raises several challenges, as shown in **Figure 2**:

- The model assembly may initially appear visually complex to new *Modelica* users.
- It requires configuring each component individually, often including low-priority or secondary parameters.
  This increases the risk of modeling errors due to incorrect settings.
- The handling of outputs becomes increasingly complex.



**Figure 2.** Component-by-Component modeling of a solar plant including a storage (TTES) loop

A first step in deploying NewLib across Newheat technical teams is to provide a user-friendly environment to it. That is the objective of the TypicalConfig package,

which is an ongoing work. The package provides different templates for typical renewable heat production plants based on subsystem models (see **Figure 3**). A plant partition into 6 subsystems has been identified including Solar Field Subsystem, Storage Subsystem, Heat Consumer Subsystem, Heat Pump Subsystem, Heat Recovery Subsystem and HLC subsystem.

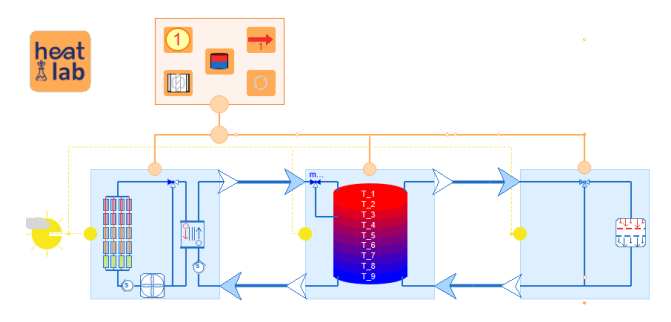


**Figure 3.** Subsystem modeling of Figure 2 Component-by-Component model of a solar plant

Each subsystem can model multiple hydraulic configurations that are commonly found in both operational plants and under development projects. For example, the solar field subsystem currently models two hydraulic configurations (see **Figure 4**):

- A direct configuration, where the solar field is directly connected to the thermal storage using a thermal oil as both the heat transfer fluid and the storage medium.
- An indirect configuration (used in Figures 2 and 3), used in all operational Newheat plants, where the thermal power from the solar field is transferred to the storage tank/user via a heat exchanger and a secondary circuit.

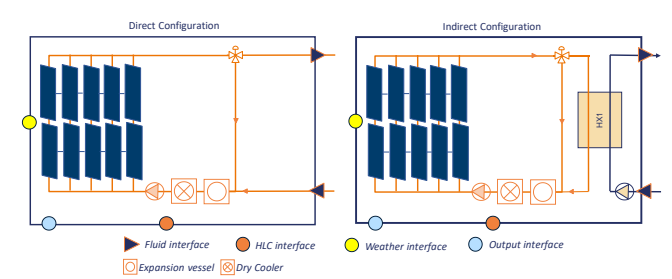


Figure 4. Hydraulic configurations of the solar field subsystem in NewLib

An error-proofing methodology is used to prevent the production of non-conforming parts in the conceptual design phase. The parameters of the subsystem components are classified into primary and secondary parameters. All primary parameters of the subsystem are defined by the user in a unique outer model called *Heatlab*. The other parameters are either pre-defined or calculated in an initial algorithm based on pre-conception rules.

The model outputs are managed using the *HideResult* annotation from *Modelica* language; KPIs (energy

balance, temperatures...) are calculated to provide a quick overview of the performances of each subsystem.

All main models of a subsystem are replaceable models, allowing for an easy switch from a conceptual design phase model, using simplified models, to a detailed engineering phase, using more complex dynamic models.

# 3 NewLib models description

This section provides a quick overview of the different models included in the NewLib library and usually used to represent large solar thermal plants. For each of these models both a conceptual design phase version and an engineering phase version are described.

### 3.1 Media models

To simulate low temperature solar thermal plants in the NewLib library, glycol water mixture (20% to 45% in volume), which is commonly used as a heat transfer fluid in those systems, is defined as a medium, with either constant properties or properties depending on the temperature of the fluid. It is considered incompressible. Polynomial equations are used to calculate the density  $(\rho)$ , heat capacity at constant pressure (cp) and thermal conductivity  $(\lambda)$ , an exponential form is used to model the dynamic viscosity  $(\mu)$  of the medium:

$$\rho = a_{d,3} \cdot T^3 + a_{d,2} \cdot T^2 + a_{d,1} \cdot T + a_{d,0} \tag{1}$$

$$cp = a_{c2}.T^2 + a_{c1}.T + a_{c0}$$
 (2)

$$\lambda = a_{l,2}.T^2 + a_{l,1}.T + a_{l,0} \tag{3}$$

$$\mu = A_e \cdot exp(B_e/(T + C_e)) \tag{4}$$

With  $a_{d,0}$ ,  $a_{d,1}$ ,  $a_{d,2}$ ,  $a_{d,3}$ ,  $a_{c,0}$ ,  $a_{c,1}$ ,  $a_{c,2}$ ,  $a_{l,0}$ ,  $a_{l,1}$ ,  $a_{l,2}$ ,  $A_e$ ,  $B_e$  and  $C_e$  being constant coefficients obtained by linear regression on fluid supplier documentation table data. If constant properties are chosen, properties of the fluid are calculated at a reference temperature defined as an input of the function. However, choosing this option can lead to significant errors in fluid pressures and/or temperatures in some cases. The main drawback of using variable properties media being larger CPU times. For specific studies during the engineering phase, hybrid media can be used. For instance, in hydraulic specification of the solar loop, constant cp,  $\lambda$  and  $\rho$  combined with variable  $\mu$  media leads to fast results and good precision on pressure losses, while thermal accuracy is not required for this phase.

### 3.2 Pipes model

In the NewLib library, a single pipe model is used for both conceptual design and engineering phase. The energy balance in pipes is calculated considering a single fluid node where heat convection from inlet to outlet is calculated in a *heatTransfertElement* component from an enthalpy balance delayed by a *TransportDelayInit* 

component that accounts for the time delay from the inlet to the outlet of the pipe:

$$M.\frac{\partial h}{\partial t} = \dot{m}.\left(h_{in} - h_{out}\right) \tag{5}$$

$$\frac{\partial h(x,t)}{\partial t} + v(t).\frac{\partial h(x,t)}{\partial x} = 0 \tag{6}$$

Where h represents the specific enthalpy of the fluid, v represents the fluid velocity, M represents the inertial mass of the metal of the pipe and  $\dot{m}$  represents the mass flow rate in the pipe. Heat losses to the external medium are calculated in a PlugFlowHeatLoss component, based on the plug flow model from IBPSA library. In this component, the outlet temperature is directly calculated from the solution of the heat equation considering only heat losses to the ambient:

$$T_{out} = T_{amb} + (T_{in} - T_{amb}). e^{-\frac{\tau}{R\rho c_p}}$$
 (7)

With  $T_{amb}$  being the ambient temperature,  $\tau$  being the residence time of the fluid in the pipe and  $R_{th}$  being the overall thermal resistance, calculated as:

$$R_{th} = \frac{2 \cdot \pi \cdot L}{\frac{1}{r_1 \cdot h_{in}} + \frac{\ln{(\frac{r_2}{r_1})}}{\lambda_{nine}} + \frac{\ln{(\frac{r_3}{r_2})}}{\lambda_{ins}} + \frac{1}{r_3 \cdot h_{out}}}$$
(8)

Where L is the pipe length,  $r_1$ ,  $r_2$  and  $r_3$  are respectively the pipe inner radius and the insulation inner and outer radius,  $h_{in}$  and  $h_{out}$  are the inner and outer convection coefficients based on literature correlations (Yang et al., 2011, The engineering Toolbox, 2003) and  $\lambda_{pipe}$  and  $\lambda_{ins}$  are the thermal conductivity coefficients of the pipe and the insulation respectively defined from pipe suppliers

For the mass balance, constant mass flow rate is considered and the pressure losses in the pipe are defined as:

$$\Delta P = \Delta P_{reg} + \Delta P_{man} \tag{9}$$

Where  $\Delta P_{reg}$  represents the regular pressure losses and is calculated considering the Darcy-Weisbach equation:

$$\Delta P_{reg} = f_D \cdot \frac{L}{D_h} \cdot \rho \cdot \frac{V^2}{2} \tag{10}$$

Where  $f_D$  is the friction factor calculated from Cheng correlations (Cheng, 2008), suitable for all flow regimes.

And  $\Delta P_{man}$  represents the manometric head, calculated as:

$$\Delta P_{man} = \rho. g. \Delta H \tag{11}$$

Where  $\Delta H$  is the height difference between the inlet and outlet of the pipe and g the constant of gravity  $g = 9.81 \, m. \, s^{-2}$ .

### 3.3 Solar field models

The conceptual design phase solar field model in NewLib represents an equivalent solar collector consisting of a single thermal and hydraulic node. It calculates an equivalent pressure loss based on a rectangular solar field layout. The thermal part considers the heat exchange with the environment and enthalpy transport considering a delay due to the residence time of the fluid in the solar field as done for the pipe model.

The detailed engineering phase model, in contrast, explicitly represents manifolds and hydraulic singularities such as elbows and restrictions. Correlations of pressure losses in these singularities and in the regular parts are used. The thermal part is equivalent to the simplified model with a level of detail at the scale of the collector row rather than the overall solar field.

For both models, the energy balance in a single collector is calculated considering the overall thermal performance equation that is based on the quasi-dynamic equation from the ISO 9806 (ISO, 2017). This equations states that the power collected by the fluid  $(P_f)$  is the difference of the absorbed heat  $(P_{abs})$  to the thermal losses  $(P_{lass})$ :

$$P_f = P_{abs} - P_{loss} (12)$$

The power absorbed by the fluid is calculated as:

$$P_{abs} = S_{col}. \, \eta_{0,b} \, . \, fc. \, (K_b(\theta_l, \theta_t) \, . \, G_b + K_d. \, G_d)$$
 (13)

Where  $S_{col}$  is the surface area of the collector,  $\eta_{0,b}$  is the optical efficiency of the collectors,  $K_b(\theta_l, \theta_t)$  and  $K_d$  are the angle of incidence factors for direct and diffuse solar irradiations respectively,  $G_b$  and  $G_d$  are direct and diffuse solar irradiations respectively. fc is the so-called cleanliness factor that considers the reduction in the solar collector's performance caused by the accumulation of dirt, dust and other deposits (more details in §4).

The thermal losses are calculated as:

$$P_{loss} = S_{col}.\begin{pmatrix} c_{1}. (T_{mf} - T_{amb}) \\ +c_{2}. (T_{mf} - T_{amb})^{2} \\ +c_{3}. u_{wind}. (T_{mf} - T_{amb}) \\ -c_{4}. (E_{L} - \sigma. T_{amb}^{4}) \\ +c_{5}. \frac{dT_{mf}}{dt} \\ +c_{6}. u_{wind}. (G_{b} + G_{d}) \end{pmatrix}$$
(14)

Where  $T_{mf}$  is the mean temperature of the fluid,  $T_{amb}$  is the ambient temperature surrounding the solar field,  $c_1$ ,  $c_2$ ,  $c_3$ ,  $c_4$ ,  $c_5$ ,  $c_6$  are respectively the heat loss coefficient, the coefficient of the temperature effect on the heat loss coefficient, the coefficient of the wind effect on the heat loss coefficient, coefficient of the sky temperature effect on the heat loss coefficient, the effective heat capacity and the coefficient of the wind effect on the optical efficiency,

given by the collector model solar Keymark (Solar Keymark Network, n.d.), which is a certification of solar thermal collectors that provides a database of their coefficients in the ISO 9806 performance equation. Both models must be connected to the NewLib weather model to get weather input. In the NewLib library, the weather model uses weather data from Newheat onsite sensors as input to a *combiTimeTable* component of the *MSL*.

For the design phase model, the mass balance considers constant mass flow rate from inlet to the outlet of the solar field and pressure losses are calculated as:

$$\Delta P_{SF} = \Delta P_{collector} + \Delta P_{piping} \tag{15}$$

Where  $\Delta P_{collector}$  and  $\Delta P_{piping}$  are the pressure losses in the collectors and the pipes respectively.

In the collectors, the pressure losses are calculated as:

$$\Delta P_{collector} = \frac{\nu(T_0)}{\nu(T)} \cdot a_0 \cdot \dot{V} + \frac{\rho(T)}{\rho(T_0)} \cdot b_0 \cdot \dot{V}^2$$
 (16)

Where  $a_0$  and  $b_0$  are respectively the collector linear and quadratic pressure loss coefficients as given by its Solar Keymark,  $\rho(T_0)$ ,  $\nu(T_0)$  and  $\rho(T)$ ,  $\nu(T)$  are the density and dynamic viscosity at reference and actual temperature respectively and  $\dot{V}$  is the volume flow rate in the collectors.

In the solar field pipes, the pressure losses are calculated as:

$$\Delta P_{nining} = \Delta P_{reg} + \Delta P_{sing} \tag{17}$$

Where  $\Delta P_{reg}$  and  $\Delta P_{sing}$  are the regular and singular pressure losses. The regular pressure losses are calculated as:

$$\Delta P_{reg} = \left(\frac{\dot{m}_{flow}}{\dot{m}_{flow,max}}\right)^2 . \Delta P_{reg,max}$$
 (18)

Where the maximal regular pressure loss in the solar field pipes is calculated from the Darcy-Weisbach equation using Cheng friction factor  $f_{D_i}$  at maximal fluid speed  $(u_{max} = 2m/s)$  in all the pipes constituting the most constraining path in the solar field:

$$\Delta P_{reg,max} = \sum f_{D_i} \cdot L_i \cdot \frac{\rho}{2} \cdot \frac{u_{max} \cdot |u_{max}|}{2 \cdot r_i}$$
(19)

$$f_{D_{i}} = \left(\frac{64}{\text{Re}_{i}}\right)^{a} \cdot \left(1.8 \cdot \log\left(\frac{\text{Re}_{i}}{6.8}\right)\right)^{2.(a-1).b} \cdot \left(2.\log\left(3.7 \cdot \frac{D_{i}}{rr}\right)\right)^{2.(a-1).(1-b)}$$
(20)

$$a = \frac{1}{\left(1 + \left(\frac{Re_i}{2720}\right)^9\right)}$$
 (21)

$$b = \frac{1}{\left(1 + \left(\frac{\operatorname{Re}_{i} \cdot rr}{320 \cdot r}\right)^{2}\right)}$$
 (22)

Where rr is the relative roughness of the pipes and  $Re_i$ ,  $L_i$ ,  $D_i$  and  $r_i$  are the Reynolds number, length, nominal diameter and internal radius, respectively, of each pipe element constituting the most constraining path.

To calculate the most constraining path in the solar field, a rectangular solar field is considered, the pipes DN are determined in an initial algorithm by targeting a maximal velocity of 2m/s in each pipe.

In the engineering phase model, the hydraulic layout of the solar field is represented in much more detail. Figure 5 shows the solar field of another large scale solar thermal plant currently under development in France, in implementation plan view and Dymola interface view of the equivalent model. The complex layout of this solar field is explained by irregular land availability. Pipes and manifolds are explicitly modeled, and regular and singular pressure losses are calculated.

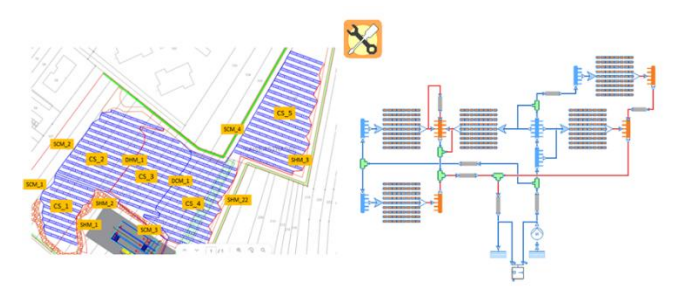


**Figure 5.** Implementation plan (left) and visualization of the equivalent model in Dymola using the NewLib library (right) of a complex solar field

**Table 1** presents the main advantages and drawbacks of each model in the NewLib library.

**Table 1.** Design and engineering phase solar field models comparison in the NewLib library

	Design phase model	Engineering phase model
Advantages	Low CPU time Easy setup	Pressure loss precision
Drawbacks	Can not be used in engineering phase	Higher CPU time

### 3.4 Pump models

368

Design phase pump model in NewLib represents a flow generator. The mass flow rate is equal to the setpoint mass flow rate as:

$$\dot{\mathbf{m}}_{flow} = \dot{\mathbf{m}}_{flow,SP} \tag{23}$$

The electricity consumption of the flow generator is then estimated as follows:

$$P_{hvd} = \Delta P.\dot{V} \tag{24}$$

$$P_{elec} = \frac{P_{hyd}}{n_{tot}} \tag{25}$$

Where  $P_{hyd}$  and  $P_{elec}$  are respectively the hydraulic and electrical powers of the pump,  $n_{tot}$  is the total efficiency of the pump as defined by the user.

The engineering phase pump model in NewLib is based on the MSL model (Modelica.Fluid.Machines.BaseClasses.PartialPump). From the characteristic curve at nominal rotational speed  $\dot{N}_{nom}$ , a polynomial function  $Pc_{nom}$  is identified:

$$H_{m \, nom} = Pc_{nom}(\dot{V}) \tag{26}$$

With  $H_{m,nom}$  being the pump head at nominal rotational speed and  $\dot{V}$  the volumetric flow rate. From this polynomial function, the pump head is deduced for every rotational speed  $\dot{N}$  and volumetric flow rate  $\dot{V}$  as:

$$H_m = \left(\frac{\dot{N}}{\dot{N}_{nom}}\right)^2 . Pc_{nom}(\dot{V}.\frac{\dot{N}_{nom}}{\dot{N}})$$
 (27)

Similarly, a polynomial function  $Pw_{nom}$  is calculated for the mechanical power of the pump from nominal values at different volume flow rates:

$$\dot{W}_{nom} = Pw_{nom}(\dot{V}) \tag{28}$$

The mechanical power of the pump  $(\dot{W})$  is then calculated for different rotational speeds  $\dot{N}$  as:

$$\dot{W} = \left(\frac{\dot{N}}{\dot{N}_{nom}}\right)^3 . Pw_{nom}(\dot{V}.\frac{\dot{N}_{nom}}{\dot{N}})$$
 (29)

The pressure loss  $(\Delta p)$  is directly deduced from the pressure head  $(H_m)$  as:

$$H_m = \frac{\Delta p}{\rho \cdot g} \tag{30}$$

Considering constant fluid density  $\rho$ .

Then, electricity consumption is evaluated from a constant combined mechanical and electrical efficiency  $\varepsilon_{elec}$ :

$$\dot{P}_{elec} = \frac{\dot{W}}{\varepsilon_{elec}} \tag{31}$$

### 3.5 Heat exchanger models

For design phase simulations, an  $\epsilon$ -NTU heat exchanger model is implemented in the NewLib library. In this model, the energy balance, constituting the heat exchange between the 2 sides of the heat exchanger is calculated from:

$$\dot{Q} = \varepsilon. \, \dot{Q}_{max} \tag{32}$$

$$\dot{Q}_{max} = C_{min} \, \Delta T_{max} \tag{33}$$

$$\Delta T_{max} = T_{h.in} - T_{c.in} \tag{34}$$

Where  $\dot{Q}$  and  $\dot{Q}_{max}$  are respectively the actual and maximal exchanged heat,  $C_{min}$  is the minimal capacity flow rate ( $c_p \cdot \dot{m}_{flow}$ ) and  $\Delta T_{max}$  is the maximal temperature difference in the heat exchanger.  $\varepsilon$  is the counter-flow configuration heat exchanger efficiency defined as:

$$\varepsilon = \begin{cases} \frac{1 - exp[-NTU \cdot (1 - R)]}{1 - R \cdot exp[-NTU \cdot (1 - R)]}, & \text{if } R < 1\\ \frac{NTU}{1 + NTU}, & \text{if } R = 1 \end{cases}$$
 (35)

With NTU (number of transfer units) defined as:

$$NTU = \frac{U.A}{C_{min}} \tag{36}$$

With *U* being the overall heat transfer coefficient and A the equivalent surface area of the heat exchanger. *R* is the heat flow rate ratio, defined as:

$$R = \frac{C_{hot}}{C_{cold}} \tag{37}$$

Where  $C_{cold}$  and  $C_{hot}$  are the capacity flow rates on the cold and hot side of the exchanger respectively. For the mass balance, constant flow rate is imposed on both sides of the heat exchanger, and pressure losses are calculated as follows:

$$p_{loss} = k_l. m_{flow} + k_q. m_{flow}$$
 (38)

Where  $k_l$  and  $k_q$  are constant coefficients defined as inputs or calculated from nominal operating point.

The engineering phase heat exchanger model in NewLib is also based on the ε-NTU method. Additional parameters are proposed to the user to define a specific heat exchanger model with the exact number of plates and other geometrical design parameters such as corrugation angle, joint thickness or expansion factor, to calculate the number of heat transfer-effective plates.

# 4 Validation and Application

### 4.1 Use case plants description

In 2019, Newheat, the city of Narbonne in the south of France and the operator of its district heating network agreed to develop a large-scale solar thermal plant to maximize the proportion of renewable energy on the network as it develops. The objective was to replace, as much as possible, the use of gas boilers with the production of solar energy, covering most of the network's needs during the summer period, from April to October. Newheat oversaw the entire project and bears full responsibility for its various stages (design, development, construction, operation for a 25-year

period). The project has received financial support from ADEME's *Fonds de Chaleur* and the Occitanie Region (France).

The solar plant project called NARBOSOL commissioned in 2021 consists of a solar field, a thermal storage tank (hot water), to offset periods of solar heat production and consumption by the heating network, and a technical room containing the programmable logic controller (PLC) and all the hydraulic equipment (pumps, valves, heat exchangers, measuring instruments, etc.). Main characteristics of NARBOSOL plant are presented in **Table 2**.

Table 2. NARBOSOL solar thermal plant main parameters.

Parameter	Value	
Location	43.183°N, 2.967°W	
Solar field aperture area (m²)	3200	
Solar field peak power (kW)	2700	
Solar collectors tilt (°)	35°	
Storage volume (m <sup>3</sup> )	1000	
Solar heat transfer fluid	Glycol 30%	
Storage fluid	Water	
Annual production (MWh)	2200	

### 4.2 Solar field Modeling

The NARBOSOL's solar field consists of 202 Savo 15 SG solar collectors (Savosolar Oyj, 2020) divided into two subsolar fields. The first subsolar field contains 12 rows, each with a range of 8 to 12 serial collectors, while the second subsolar field contains 7 rows, each with a range of 7 to 10 serial collectors (see **Figure 6**). Both subsolar fields are connected to the hydraulic skid from a cold and a hot manifold to feed all the rows with the heat transfer fluid. Balancing valves are used to equally distribute the system's total flow in each row as a function of serial collector number.



**Figure 6.** Aerial view of NARBOSOL solar thermal plant in Narbonne (France)

Newheat uses remotely accessible supervision technologies to monitor the plant's status and modify its parameters to maintain optimal operating conditions. All data transmitted from the sensors (temperature, pressure,

mass flow, electric consumption...) installed in NARBOSOL are recorded with a time step of 1 min in a proprietary data base. In this paper, data recorded in 2024 at NARBOSOL is used to compare the performance of both approaches in modeling the solar field and other components of the solar loop in NewLib, dedicated to the conceptual design phase and the detailed engineering phase.

### Evaluation of the cleanliness factor of NARBOSOL

The cleanliness factor fc (see **Equation (13)**) of a solar field model is a parameter that affects the optical efficiency of the collectors by reducing the incident solar power.

To assess the annual mean cleanliness factor value of NARBOSOL plant, an assembly model was developed. It includes the conceptual design phase model of the solar field and other physical components such as pumps and pipes from the NewLib library. One-minute frequency measurements of weather data (Global Tilted Irradiation-GTI, wind speed, and ambient temperature), volume flow rate, and inlet temperature are used as inputs of the model. The model calculates the 8760 hourly thermal power delivered to the fluid by the solar field in 2024. **Figure 7** shows the graphical representation of this assembly model in the *Dymola* environment.

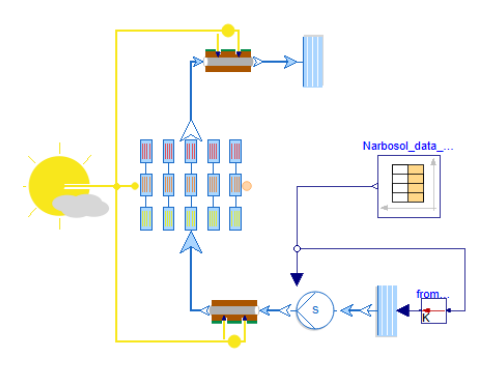


**Figure 7.** Graphic view of the design phase model of NARBOSOL's solar field in NewLib

A parametric study is then carried out using this assembly model, in which the root means square error (RMSE) is computed by comparing the model results with the measured thermal power as a function of the cleanliness factor.

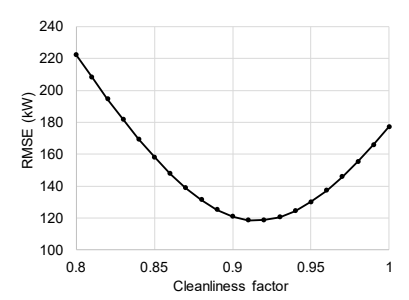


**Figure 8.** Parametric study for the evaluation of the cleanliness factor

**Figure 8** presents the results of this parametric study. The graph clearly shows the value of the cleanliness factor of 92 % that minimizes the RMSE.

### Solar field models evaluation

In this section, the performance of both NewLib solar field models (§3.3) is evaluated. To do so, 2 assembly models of the NARBOSOL plant, similarly to **Figure 7**, are developed using NewLib library's conceptual design phase models and engineering phase models. Simulations are carried out using these 2 assembly models on 1-minute step data from September 2024 at NARBOSOL.

The results are compared with the measurements from September 2024 in terms of monthly cumulative energy (**Figure 9**), thermal power (**Figure 10**), and hydraulic characteristic curve of the solar field (**Figure 11**). For both models, the value of the cleanliness factor of 92 % determined in the previous section is used. The 30% glycol water medium with variable properties (see §3.1) is used in both simulations.

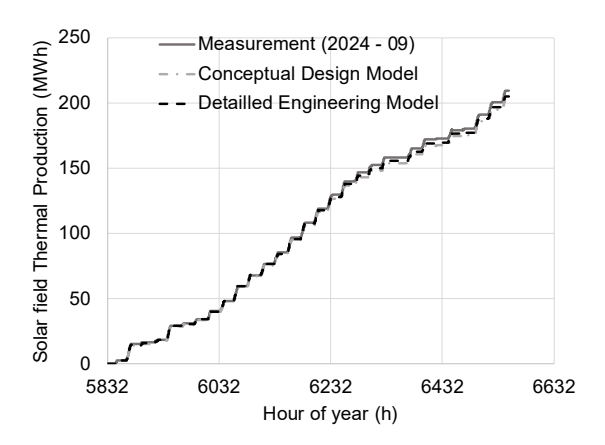


**Figure 9.** Cumulative Energy provided by the solar field in September 2024

Figure 9 shows a very good agreement between both models and measurement. In September 2024, the energy delivered to the fluid by the NARBOSOL solar field was measured at 209.4 MWh, while the calculated values were 202.9 MWh (3% error) and 205.0 MWh (2% error) for the conceptual design model and the detailed engineering model, respectively. These results suggest that the level of detail at the overall solar field scale used in the conceptual design model is sufficient to accurately represent the thermal performances of large-scale solar fields. Better agreement between measured and simulated data in the first half of the month can be explained by sunnier days during this period. The model being more accurate when less irradiation variations.

**Figure 10** further confirms this result in terms of thermal power on two chosen cloudy and sunny days. Finaly, this graph strengthens the observation that the conceptual design model provides a very good estimation of the solar field's thermal performance despite its simplified level of detail. The correlation coefficient over the whole month

on solar field thermal power is 0.9904 for the conceptual phase model compared to 0.9908 for the more detailed one.

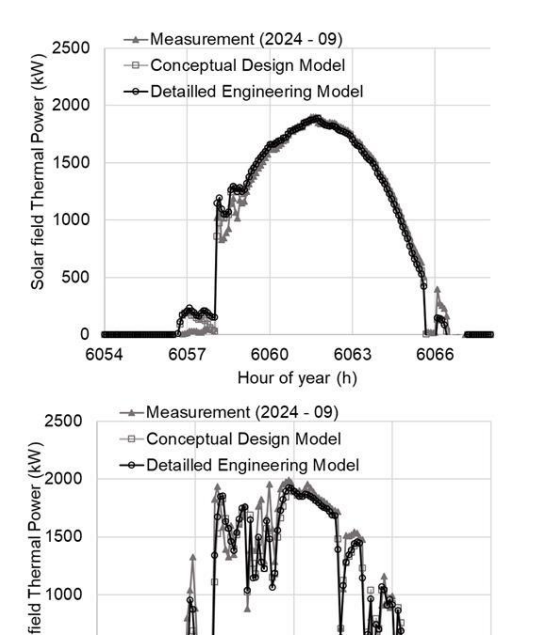


**Figure 10.** Solar thermal power result comparison between both models and measured data for a sunny day (top) and a cloudy day (bottom)

Hour of year (h)

6113

Solar 1

6104

However, results on the solar field pressure drop (see Figure 11) show that the conceptual design model is unable to predict the hydraulic behavior of the solar field. In the case of NARBOSOL's model, this result is due to the estimation of the most constraining path in the solar field, based on the assumption of a rectangular solar field, which is far from the real configuration in this case. In the detailed engineering model, the hydraulic layout of the solar field is represented in much more detail, including pipes, manifolds and a refined representation of each subsolar field with the actual number of collectors in series for each row. As shown in Figure 11, this level of detail enables highly accurate results on pressure loss prediction.

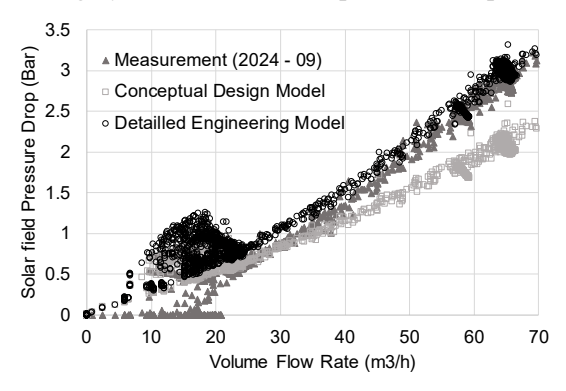


**Figure 11.** Hydraulic characteristic curve of the solar field for both model representations and measured data

### Solar field complete loop modeling

In this final section, NewLib's detailed engineering models are integrated within a larger Component-by-Component assembly model of the solar field loop, which includes:

- A centrifugal pump model (see §3.4), a heat exchanger model (see §3.5), a singular pressure drop model of the hydraulic skid, and other standard models of hydraulic components such as a 3-ways valve and an expansion vessel.
- The HLC model which calculates the operating modes of the solar field loop (§2.2).
- LLC Models of the solar field, valve, pump and heat exchanger which determines the commands to be sent to reach the HLC model setpoints.

The centrifugal pump model is based on the technical specifications of the ETL 065-065-160 pump from KSB. It defines the pump head and the shaft power as a function of rotation speed and volume flow rate. Then a constant combined mechanical and electrical efficiency of 0.95 x 0.95 x 0.95 is assumed, which reflects losses in the pump/electric motor coupling, frequency inverter, and electric motor. The heat exchanger model is based on a nominal operating point defined by inlet/outlet temperatures of 91.2 °C / 67.1 °C on the primary side and 63 °C / 88.5 °C on the secondary side, with an exchanged thermal power of 1.9 MW. **Figure 12** presents a visualization of the described assembly model in the *Dymola* environment.

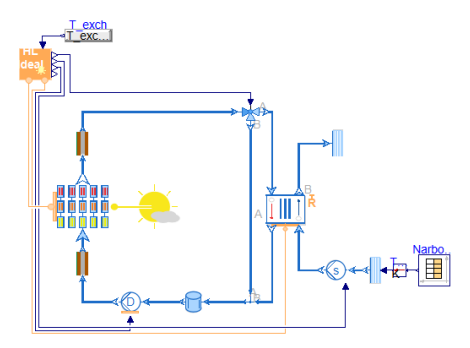


**Figure 12.** Model of NARBOSOL's solar field loop in NewLib as seen in Dymola

A simulation is launched on 1-minute frequency weather and inlet temperature of the secondary loop data in September 2024 at NARBOSOL, as inputs of the model. Results of heat power comparison are presented in **Figure 13** for a cloudy day. A very good agreement between simulation and measurement data is observed. The correlation coefficient is 0.9769 over the whole month.

**Table 3** shows measured and simulated September 2024 energy balances in the solar loop. Regarding thermal energy, the deviation is limited, with a 2% difference between calculated and measured values.

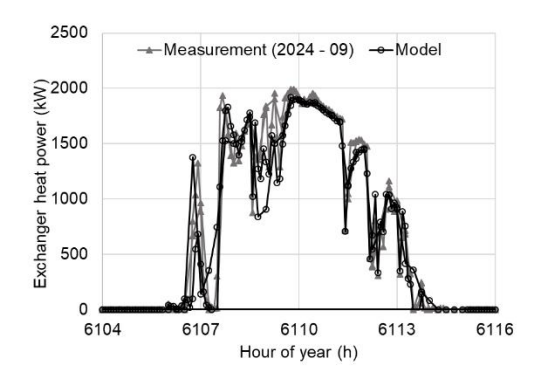


**Figure 13.** Heat supplied to the tank result comparison between both models and measured data

The centrifugal pump electrical consumption is also well estimated, with a deviation of 11 % compared to the measurements. This higher deviation in the pump electrical consumption can be partly attributed to differences between the actual equipment and its technical specifications.

**Table 3:** Energy balance comparison for September 2024 between both models and measured data

	Measurements	Model
Thermal solar Energy	209.4 MWh	211.8 MWh
Energy provided to storage	207.4 MWh	212.5 MWh
Electric pump consumption	1.8 MWhe	2.0 MWhe

### 5 Conclusion

In this paper, the 2 different modeling approaches available in the NewLib library are presented. Comparisons of these 2 modeling approaches with measured data on an operating solar plant have been carried out.

On the one hand, the conceptual design phase model of the solar field in NewLib provides robust thermal results but cannot be used for hydraulic conception purpose during the engineering phase of projects due to its lack of accuracy in pressure losses prediction. On the other hand, the detailed solar field model offers significantly improved accuracy in pressure loss calculations and combined with medium representation can lead to acceptable simulation time. The NARBOSOL case serves as a prime example of these advantages.

Future perspectives of this work for each phase of Newheat projects are:

• Conceptual design phase: Finalization of the template-based approach to streamline model development.

- Engineering phase: Development of detailed models for key components, including heat exchangers and valves, to enhance system accuracy.
- Operational phase: Refinement of detailed models to facilitate the implementation of a digital twin approach, ultimately optimizing maintenance operations, such as fault detection like leak identification, and improving overall system performance.

These advancements pave the way for more accurate simulations and the potential for real-time optimization in future applications.

# Acknowledgements

This work has been supported by ADEME and Région Nouvelle Aquitaine (France). The authors would also like to thank *TFS* developers for their work.

### References

Cheng, Nian-Sheng, 2008. Formulas for Friction Factor in Transitional Regimes, Journal of Hydraulic Engineering. 134 (9): 1357–1362. doi:10.1061/(asce)0733-9429(2008)134:9(1357). hdl:10220/7647. ISSN 0733-9429.

Hammond-Scott, H., 2022. Testing Library: A look Inside. Claytex, URL https://www.claytex.com/tech-blog/testing-library-a-look-inside/ (visited on 2025-4-28). International Organization for Standardization, 2017. ISO

9806:2017: Solar Energy — Solar Thermal Collectors — Test Methods.

Olsson, H. 2020, URL https://github.com/HansOlsson/Modelica\_StateGraph2 (visited on 2025-4-28).

Savosolar Oyj, 2020. Savo 15 SG-M collector – Technical datasheet. https://meriauragroup.com/wp-content/uploads/archive/savosolar.com/wp-content/uploads/Savo-15-SG-M-technical-datasheet-2020-03-26-EN.pdf (visited on 2025-04-29).

Solar Keymark Network. (n.d.). Solar Keymark Certification Scheme. Retrieved from <a href="https://solarheating.eu/solar-keymark/">https://solarheating.eu/solar-keymark/</a>.

The Engineering ToolBox, 2003. Understanding Convective Heat Transfer: Coefficients, Formulas & Examples. [online]: https://www.engineeringtoolbox.com/convective-heat-transfer-d 430.html (visited on 2023-08-29).

Wetter, M., 2022. URL https://github.com/ibpsa/modelica-ibpsa/wiki (visited on 2025-4-28).

Yang, J-K et al., 2011. Heat Transfer Coefficient in Flow Convection of Pipe-Cooling System in Massive Concrete. Journal of Advanced Concrete Technology 9, no 1:103-104.

Zimmer, D., 2020. Robust object-oriented formulation of directed thermofluid stream networks. Mathematical and Computer Modelling of Dynamical Systems 26, 204–233. https://doi.org/10.1080/13873954.2020.1757726.

Zimmer, D., Meißner, M., Weber, N., 2022. The DLR ThermoFluid Stream Library. Electronics 11, 3790. https://doi.org/10.3390/electronics11223790.